



Estimating C_4 photosynthesis parameters by fitting intensive A/C_i curves

Haoran Zhou¹ · Erol Akçay¹ · Brent R. Helliker¹

Received: 22 October 2018 / Accepted: 21 January 2019 / Published online: 13 February 2019
© Springer Nature B.V. 2019

Abstract

Measurements of photosynthetic assimilation rate as a function of intercellular CO_2 (A/C_i curves) are widely used to estimate photosynthetic parameters for C_3 species, yet few parameters have been reported for C_4 plants, because of a lack of estimation methods. Here, we extend the framework of widely used estimation methods for C_3 plants to build estimation tools by exclusively fitting intensive A/C_i curves (6–8 more sampling points) for C_4 using three versions of photosynthesis models with different assumptions about carbonic anhydrase processes and ATP distribution. We use simulation analysis, out of sample tests, existing in vitro measurements and chlorophyll-fluorescence measurements to validate the new estimation methods. Of the five/six photosynthetic parameters obtained, sensitivity analyses show that maximal-Rubisco-carboxylation-rate, electron-transport-rate, maximal-PEP-carboxylation-rate, and carbonic-anhydrase were robust to variation in the input parameters, while day respiration and mesophyll conductance varied. Our method provides a way to estimate carbonic anhydrase activity, a new parameter, from A/C_i curves, yet also shows that models that do not explicitly consider carbonic anhydrase yield approximate results. The two photosynthesis models, differing in whether ATP could freely transport between RuBP and PEP regeneration processes yielded consistent results under high light, but they may diverge under low light intensities. Modeling results show selection for Rubisco of low specificity and high catalytic rate, low leakage of bundle sheath, and high PEPC affinity, which may further increase C_4 efficiency.

Keywords A/C_i curves · C_4 · Estimation method · Non-linear curve fitting · Photosynthesis parameters · V_{cmax} · Electron transport · PEP carboxylation rate · Carbonic anhydrase

Abbreviations

a	Light absorptance of leaf
A_c	Rubisco carboxylation assimilation rate
$RCPC$	RuBP carboxylation and PEPc carboxylation limitation assimilation
$RrPc$	RuBP regeneration and PEP carboxylation limitation assimilation

A_g	Gross CO_2 assimilation rate per unit leaf area
A_j	RuBP regeneration assimilation rate
A_n	Net CO_2 assimilation rate per unit leaf area
$RcPr$	RuBP carboxylation and PEPc regeneration limitation assimilation
$RrPr$	RuBP regeneration and PEPc regeneration limitation assimilation
α	The fraction of O_2 evolution occurring in the bundle sheath
c	Scaling constant for temperature dependence for parameters
CaL	Lower boundary CO_2 under which assimilation is limited by RuBP carboxylation and PEPc carboxylation
CaH	Higher boundary CO_2 above which assimilation is limited by RuBP regeneration and PEPc regeneration
C_{bs}	Bundle sheath CO_2 concentration
C_i	Intercellular CO_2 concentration
C_m	Mesophyll CO_2 concentration

Electronic supplementary material The online version of this article (<https://doi.org/10.1007/s11120-019-00619-8>) contains supplementary material, which is available to authorized users.

✉ Haoran Zhou
haoranzh@sas.upenn.edu

Erol Akçay
eakcay@sas.upenn.edu

Brent R. Helliker
helliker@sas.upenn.edu

¹ Department of Biology, University of Pennsylvania, 433 S University Ave., 314 Leidy Labs, Philadelphia, PA 19104, USA

ΔH_a	Energy of activation for temperature dependence for parameters
ΔH_d	Energy of deactivation for temperature dependence for parameters
ΔS	Entropy for temperature dependence for parameters
ϕ_{PSII}	Quantum yield
$\gamma^*(25)$	The specificity of Rubisco at 25 °C
g_{bs}	Bundle sheath conductance for CO ₂
g_{bso}	Bundle sheath conductance for O ₂
g_{m}	Mesophyll conductance for CO ₂
I	Light intensity
$J(25)$	Maximum rate of electron transport at 25 °C at a specific light intensity
$J_{\text{max}}(25)$	Maximum rate of electron transport at 25 °C
$K_c(25)$	Michaelis–Menten constant of Rubisco activity for CO ₂ at 25 °C
$K_o(25)$	Michaelis–Menten constants of Rubisco activity for O ₂
$K_p(25)$	Michaelis–Menten constants of PEP carboxylation for CO ₂
O_{bs}	O ₂ concentration in the bundle sheath cells
Q_{10} for K_p	Temperature sensitivity parameter for K_p
R	The molar gas constant
R_d	Daytime respiration
R_{dbs}	Daytime respiration in bundle sheath cells
R_{dm}	Daytime respiration in mesophyll cells
Rubisco	Ribulose-1,5-bisphosphate carboxylase/oxygenase
RuBP	Ribulose-1,5-bisphosphate
T_k	Leaf absolute temperature
V_c	Velocity of Rubisco carboxylation
$V_{\text{cmax}}(25)$	Maximal velocity of Rubisco carboxylation at 25 °C
V_p	PEP carboxylation
V_{pc}	PEPc reaction rate
$V_{\text{pmax}}(25)$	Maximal PEP carboxylation rate at 25 °C
V_{pr}	PEP regeneration rate
x	The maximal ratio of total electron transport could be used for PEP carboxylation

Introduction

Key photosynthetic parameters allow for the assessment of how biochemical and biophysical components of photosynthesis affect net carbon assimilation in response to environmental changes, phenotypic/genotypic differences, genetic modification, and the evolution of photosynthesis pathway. The changes in net assimilation (A_n) that occur along with the changes of intercellular CO₂ concentration (C_i)—or A/C_i curves—are widely used to estimate photosynthetic parameters for C₃ species. In particular, the method

by Sharkey et al. (2007), based on the C₃ photosynthesis model of Farquhar et al. (1980; FvCB model), has been one of the most widely used tools since it is based exclusively on A/C_i curves, which are easy to measure in both lab and field conditions.

Fewer estimates of photosynthetic parameters have been reported for C₄ species, as there has been a lack of accessible C₄ estimation methods. C₄ photosynthesis enables the concentration of CO₂ around Rubisco, thus reducing photorespiration. The concentration mechanism requires the carbonic anhydrase and PEP carboxylation/regeneration processes to operate. Furthermore, the enzymes which decarboxylate C₄ acids in the PEP regeneration differ and result in three different C₄ subtypes. The tight bundle sheath wall, which prevents CO₂ from diffusing out from the bundle sheath, also limits the diffusion of gaseous CO₂ into and O₂ out of the photosynthesis spot. To model such a concentration mechanism requires accounting for distinct biochemistry and morphology, which leads to increased complexity in estimating parameters for C₄ photosynthesis. Despite this, several recent studies used A/C_i curves to estimate photosynthesis parameters based on the C₄ photosynthesis model of von Caemmerer (2000) (Ubierna et al. 2013; Bellasio et al. 2015). These studies use partial A/C_i curves; measuring assimilation rates for only a few CO₂ concentrations coupled with ancillary measurements of chlorophyll fluorescence and/or 2% O₂. While these estimation methods lead to estimates of photosynthetic parameters, the additional measurements they require make estimation more cumbersome for field work or large-scale sampling. Theoretically, it is possible to estimate photosynthetic parameters by exclusively fitting A/C_i curves to a C₄ photosynthesis model. In this paper, we propose a method to estimate C₄ photosynthesis parameters using only A/C_i curves.

There are several potential problems with A/C_i -based estimation methods for C₃ plants that carry over to existing C₄ methods (Gu et al. 2010); it is therefore important to develop a C₄ estimation method with improvements to solve the general problems and drawbacks outlined below. First, the structure of the FvCB model makes it easy to be over-parameterized. Second, a general shortcoming for the estimation methods is that they require an artificial assignment of the RuBP regeneration and Rubisco carboxylation limitation states to parts of the A/C_i curves (Xu and Baldocchi 2003; Ethier et al. 2006; Ubierna et al. 2013; Bellasio et al. 2015), which has turned out to be problematic (Type I methods) (Gu et al. 2010). These methods assume constant transition points of limitation states for different species. Furthermore, Type I methods tend to minimize separate cost functions of different limitation states instead of minimizing a joint cost function. Some recent estimation methods for C₃ species ameliorate these problems by allowing the limitation states to vary at each iterative step of minimizing

the cost function (Type II methods; Dubois et al. 2007; Miao et al. 2009; Yin et al. 2009; Gu et al. 2010). However, for these type II methods, additional degrees of freedom in these “auto-identifying” strategies can lead to over-parameterization if limitation states are allowed to change freely for all data points. Gu et al. (2010) also pointed out that existing Type I and Type II methods fail to check for inadmissible fits, which happen when estimated parameters lead to an inconsistent identification of limitation states from the formerly assigned limitation states. More specifically to C_4 , the recently developed C_4 estimation methods artificially assign limitation states for A/C_i curves (Ubierna et al. 2013; Bellasio et al. 2015) and also did not check for inadmissible fits.

Here, we present a method to estimate photosynthetic parameters for C_4 species based solely on fitting intensive A/C_i curves to a C_4 photosynthesis model (von Caemmerer 2000). Using intensive A/C_i curves (with 6–8 more sampling points than the commonly used for C_3 species) for C_4 plants is important for two reasons: First, at low C_i , the slope of A/C_i is very steep and the assimilation rate saturates quickly. Second, C_4 species have more photosynthetic parameters as the carbon concentrating mechanism adds complexity. A further complication arises due to the fact that carbonic anhydrase catalyzes the first reaction step for C_4 photosynthesis (Jenkins et al. 1989). It has been commonly assumed to not limit CO_2 uptake in estimation methods and C_4 models (von Caemmerer 2000; Yin et al. 2011b). Recent studies, however, showed evidence of potential limitation by carbonic anhydrase (von Caemmerer et al. 2004; Studer et al. 2014; Boyd et al. 2015; Ubierna et al. 2017).

To address these issues we first build an estimation method using two different fitting procedures of Sharkey et al. (2007) and Yin et al. (2011b) without considering carbonic anhydrase activity. Then, we add carbonic anhydrase limitation into the estimation method. This allows us to also use our method to examine how the carbonic anhydrase-limitation assumption impacts parameter estimation, and whether the modeling of C_4 photosynthesis can be simplified by omitting it. All together, our method estimates five to six photosynthesis parameters: (1) maximum carboxylation rate allowed by ribulose 1,5-bisphosphate carboxylase/oxygenase (Rubisco) (V_{cmax}), (2) rate of photosynthetic electron transport (J), (3) day respiration (R_d), (4) maximal PEP carboxylation rate (V_{pmax}), (5) mesophyll conductance (g_m), and optionally (6) the rate constant for carbonic anhydrase hydration activity (k_{CA}). Our approach eliminates common problems occurring in the previous C_3 and C_4 estimation methods in the following ways. First, we avoid over-parameterization, maximizing joint cost function, freely determining transition points instead of assigning in advance, and checking for inadmissible fits. Second, since both RuBP regeneration and PEP regeneration need ATP (Hatch 1987), we also

examine two different assumptions about ATP distribution between RuBP regeneration and PEP regeneration in C_4 photosynthesis models. Third, we validate the estimation methods in four independent ways, using: (i) simulation tests using A/C_i curves generated using our model with known parameters and adding random errors, (ii) out of sample test, (iii) existing in vitro measurements, and (iv) chlorophyll fluorescence measurements. Finally, we use the C_4 photosynthesis model to perform sensitivity analyses and simulation analyses for important physiological input parameters.

Materials and methods

C_4 mechanism

The CO_2 concentrating mechanism of C_4 pathway increases CO_2 in the bundle sheath cells to eliminate photorespiration. Like the C_3 pathway, the diffusion of CO_2 starts from the ambient atmosphere through stomata into intercellular spaces, and then into the mesophyll cells. In the mesophyll cells, the first step is the hydration of CO_2 into HCO_3^- by carbonic anhydrase. PEPC, then, catalyzes HCO_3^- and PEP into C_4 acids and the C_4 acids are transported to the bundle sheath cells. In the bundle sheath cell, C_4 acids are decarboxylated to create a high CO_2 environment for the C_3 photosynthetic cycle, and PEP is regenerated. All the modeling equations and mechanistic processes used for our estimation method are from von Caemmerer (2000), Hatch and Burnell (1990), Boyd et al. (2015) and Ubierna et al. (2017) (Supplementary Methods).

Given the two limitation states of C_4 cycle (PEP carboxylation (V_{pc}) and PEP Regeneration (V_{pr})), and two limitation states of C_3 cycle (RuBP carboxylation (A_c) and RuBP Regeneration (A_j)) in the C_4 photosynthesis model, there are four combinations of limitation states (as Yin et al. 2011b, Fig. 1): RuBP carboxylation and PEP carboxylation limited assimilation (RcPc), RuBP carboxylation and PEP regeneration limited assimilation (RcPr), RuBP regeneration and PEP carboxylation limited assimilation (RrPc), and RuBP regeneration and PEP regeneration limited assimilation (RrPr) (Table 1). Since the C_4 cycle operates before the C_3 cycle and provides substrates for the C_3 cycle, the determination process of A_n is as follows:

$$\text{If } (V_{pc} < V_{pr}), A_c = RcPc, A_j = RrPc, \text{ otherwise} \\ A_c = RcPr, A_j = RrPr \quad (1)$$

$$A_n = \min(A_c, A_j), \quad (2)$$

which we used for our estimation method.

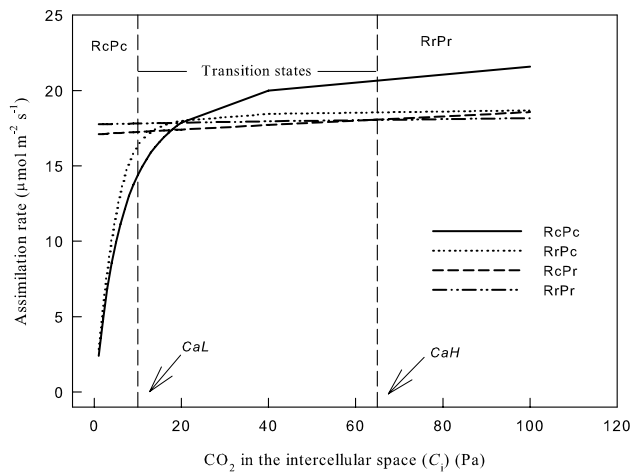


Fig. 1 An introduction of how our estimation methods assign transition points between limitation states. RcPc represents RuBP carboxylation, and PEP carboxylation limited assimilation rate, RrPr represents RuBP regeneration and PEP regeneration limited assimilation rate. Transition states indicate assimilation could be limited by RcPc, RrPr, RcPr (RuBP carboxylation and PEP regeneration), and RrPc (RuBP regeneration and PEP carboxylation). Our algorithm allows the transition states to be freely limited by the above four conditions from a lower bound (*CaL*, 10 Pa for instance) and a higher bound (*CaH*, 65 Pa for example), indicated by the dashed vertical lines in the figure

Plant material

We performed intensive A/C_i curves on nine different C_4 species to develop and examine the efficacy of our estimation tools in the greenhouse of University of Pennsylvania (elevation of 13 m): *Zea mays* L., *Eragrostis trichodes* (Nutt.) Alph. Wood, *Andropogon virginicus* L., *Schizachyrium scoparium* (Michx.) Nash, *Panicum virgatum* L., *Panicum amarum* Elliott, *Setaria faberi* Herrm., *Sorghastrum nutans* (L.) Nash, and *Tripsacum dactyloides* (L.) L. The intensive A/C_i curves contain more sample points under more CO_2 concentrations than the default curve used for C_3 species. Here we set the CO_2 concentrations as 400, 200, 50, 75, 100, 125, 150, 175, 200, 225, 250, 275, 300, 325, 350, 400, 500, 600, 700, 800, 1000, 1200, 1400 ppm under light intensity of $1500 \mu\text{mol m}^{-2} \text{s}^{-1}$ (light intensity encountered by the plants in greenhouse). At each point, data were recorded when the intercellular CO_2 concentration equilibrated within 2–5 min.

Table 1 Acronyms, detailed descriptions and applied conditions for the four limitation states of C_4 photosynthesis process

Acronyms	Limitation states	Condition
RcPc	RuBP carboxylation and PEP carboxylation limited assimilation	Low C_i
RcPr	RuBP carboxylation and PEP regeneration limited assimilation	Intermediate C_i
RrPc	RuBP regeneration and PEP carboxylation limited assimilation	Intermediate C_i
RrPr	RuBP regeneration and PEP regeneration limited assimilation	High C_i

The datasets were obtained using a standard $2 \times 3 \text{ cm}^2$ leaf chamber with a red/blue LED light source of LI-6400 (LI-COR Inc., Lincoln, NE, USA). If the stomatal conductance of a species does not decrease quickly at high CO_2 , then more points can be obtained by increasing the CO_2 level. Fluorescence was measured along with A/C_i curves for seven C_4 species (CO_2 concentration is similar with above). After each change of CO_2 concentration and A reached steady state, the quantum yield was measured by multiphase flash using a 2 cm^2 fluorescence chamber head (Bellasio et al. 2014). All the measurements were conducted at a leaf temperature of $25 \text{ }^\circ\text{C}$ and VPD was controlled at 1–1.7 kPa with the flow rate of $500 \mu\text{mol s}^{-1}$. The cuvette was covered by Fun-Tak to avoid and correct for the leakiness (Chi et al. 2013).

Estimation protocol

We implemented the estimation methods using the non-linear curve fitting routine in MS Excel (Supplementary Material I, II, III) and independently in R (“C4Estimation”) to get solutions that minimize the squared difference between observed and predicted assimilation rates (A). Five (or six when considering carbonic anhydrase) parameters will be estimated by fitting the A/C_i curve: V_{cmax} , J , R_d , V_{pmax} , g_m , and k_{CA} . Other input parameters for C_4 are in Table S1.

Input data sets and preliminary calculations

The input data sets are the leaf temperature during measurements, atmosphere pressure, two CO_2 bounds (*CaL* and *CaH* discussed in the following section), and the assimilation rates (A) and the C_i s (in ppm) in the A/C_i curve. Also, reasonable initial values of output parameters need to be given in the output section to initiate the non-linear curve fitting (Supplementary Material IV). C_i will be adjusted from the unit of ppm to the unit of Pa inside the program as suggested by Sharkey et al. (2007).

Estimating limitation states

We set upper and lower limits to the value of C_i between which the assimilation rates are freely determined by limitation states. We further avoid over-parameterization by pre-assigning limitation states at the lower and upper ends of

the C_i range. Specifically, we assume that under very low C_i (CaL), CO_2 is the limiting substrate; thus, V_p is limited by V_{pc} and A is given by A_c (RcPc); under very high C_i (CaH) electron transport is limiting, thus, V_p is limited by V_{pr} and A is given by A_j (RrPr) (Fig. 1). The points between CaL to CaH are freely determined by RcPc, RcPr, RrPc, or RrPr from Eqs. (3) to (4) to minimize the cost function. We recommend setting CaL as 10 Pa initially, then adjusting based on the preliminary results. The points of constant A at high C_i end can initially be set as being limited by RrPr primarily (based on the three points, we can CaH) or use 65 Pa as the first trial. The range of freely determined points can be adjusted by users by setting appropriate CaL and CaH . In the column of “Estimate Limitation”, whether the data points are limited by RcPc (represented by “1”), RrPr (represented by “4”), or freely vary (represented by “0”), all the assignments of “1”, “4”, and “0” are determined automatically by the given values of CaL and CaH . One can input “– 1” to disregard a data pair. Users can adjust limitation states according to how many points and the range of C_i they have in their A/C_i curves.

We assume different processes in the C_4 photosynthesis are coordinated with each other and co-limit the assimilation rate (Sharkey et al. 2007; Yin et al. 2011b; Ubierna et al. 2013; Bellasio et al. 2015). Thus, the estimation parameters allow the limitation states to be compactly clustered with each other (Fig. 1). However, if there were only a few points under CaL , the estimation results will depend heavily on the given initial values and unbalanced results would be more likely. Fig. S1 shows an example of unbalanced estimation results by deleting some points under 10 Pa or setting a very low CaL : in the estimation results, A_n is limited by $RcPc$ at very low C_i and is mostly limited by A_j (shown by RrPc and RrPr) in the C_3 cycle. In this case, A_c (shown by RcPc and RcPr) has a clear redundancy at higher C_i . Unbalanced results happened when there are not enough constraints points under CaL or above CaH . Such results explain why intensive A/C_i curves are preferred, especially more measuring points under the lower end and higher end of C_i . However, existing A/C_i data with 14 points might be used in the current estimation method if there are at least four points below CaL and three points above CaH .

Estimation algorithm and fitting procedures

The objective of our estimation methods is to minimize the following joint cost function (Eqs. 3 and 4) by varying the above five or six output parameters (V_{cmax} , J , R_d , V_{pmax} , g_m , and k_{CA}):

$$f = \sum_{(i=1)}^n (A_i - A_{mi})^2, \tag{3}$$

$$A_i = [If(C_i \leq CaL), RcPc; If(C_i \geq CaH), RrPr; IF(CaL \leq C_i \leq CaH), \min(A_{ci}, A_{ji})] \tag{4}$$

n is the total number of observations, A_{ci} is determined by RcPc and RcPr and A_{ji} is determined by RrPc and RrPr from Eq. (1), A_{mi} is the observed net assimilation rate.

In this calculation, we take Michaelis–Menten constant of Rubisco activity for CO_2 (K_c), Michaelis–Menten constant of Rubisco activity for O_2 (K_o), the specificity of Rubisco (γ^*), Michaelis–Menten constants of PEP carboxylation for CO_2 or HCO_3^- (K_p), the fraction of O_2 evolution occurring in the bundle sheath (α), and bundle sheath conductance (g_{bs}) as given (input parameters), similar to Sharkey et al. (2007). We conduct further sensitivity analyses in the following section to determine the effects of variability of these inputs parameters on the estimation results.

We used two fitting procedures in the current study: one was from Sharkey et al. (2007), which is an implicit minimization of error (Supplementary Material I, III), and the other one was based on the explicit calculations given by Yin et al. (2011b) (Supplementary Material II). For the method of Sharkey et al. (2007), “estimated” A_n was calculated using the above equations and observed A_n values. We call them “estimated”, because when we calculate A_n , observed A_n is used to calculate intermediate parameters, for example, the CO_2 concentration in mesophyll cells (C_m), the CO_2 concentration in bundle sheath (C_{bs}), which we then use to calculate A_c and A_j . The objective function is to minimize the sum of square errors between “estimated” A_n and observed A_n (Simulation Error in Supplementary Material I, III). For the model without carbonic anhydrase, Yin et al. (2011b) gave explicit solutions for RcPc, RcPr, RrPc, and RrPr. “Explicit” here means the assimilation rates are totally calculated by the estimated parameters without calculating the intermediates with observed A_n . These calculations give us the real estimation error of our fitting procedure for models without carbonic anhydrase and thus provide a validation for the goodness of fit (“True Error” in Supplementary Material I-III).

Checking inadmissible fits

We made it possible to check the inadmissible fits for limitation states in our estimation method. After the estimation process finishes, the limitation states based on the estimated parameters are calculated in the last column. If the calculated limitation states are inconsistent with the assigned ones in the estimation method, one needs to readjust the assignment of the “Estimate Limitation” (adjust CaL or CaH) and rerun the estimation method, until they are consistent with each other.

Results

Estimation results and assumptions

Estimation methods based on assumptions with and without carbonic anhydrase yield similar results (Supplementary material V). In Supplementary material III, carbonic anhydrase indeed shows limitation to V_{pc} , which confirms its potential role as a limiting step in the C_4 cycle. However, V_{pc} calculated from CO_2 are only a little higher than V_{pc} calculated from HCO_3^- , which resulted in the similar estimation results. In addition, the estimation errors and true errors from Yin's equations are quite small (average < 1), and also similar between models with and without carbonic anhydrase.

Estimation methods based on the two equations of different assumptions about electron transport between RuBP regeneration and PEP regeneration yield consistent parameter estimates and assimilation- CO_2 response curves (Fig. 2), but there were minor differences. The second assumption that ATP, resulting from electron transport, is freely allocated between PEP carboxylation-regeneration and RuBP regeneration leads to a bump at low CO_2 when estimating RcPr. The two assumptions produce different RcPr under

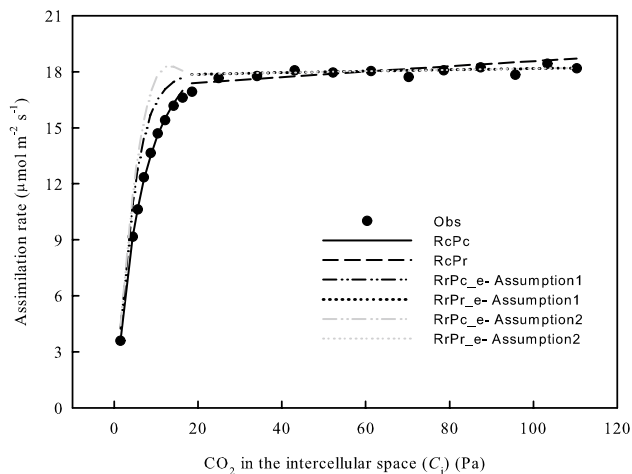


Fig. 2 Assimilation- CO_2 response curves (A/C_i) generated using C_4 photosynthesis of two different assumptions about electron transport. Photosynthetic parameters (V_{cmax} , J , R_d , V_{pmax} , and g_m) are the same for both assumptions. RrPc_e-Assumption1 and RrPr_e-Assumption1 represent results of the assumption that no matter how much electron transport is used for PEP carboxylation/regeneration, a certain amount ($\times J$) is confined for this use. RrPc_e-Assumption2 and RrPr_e-Assumption2 represent results of the assumption that electron transport can be freely distributed between PEP carboxylation/regeneration and RuBP regeneration. Parameters are estimated from A/C_i curve of *T. dactyloides* under the light intensity of $1500 \mu mol m^{-2} s^{-1}$. RcPc and RcPr are the same for both assumptions

low CO_2 ; but this is largely inconsequential because, under low CO_2 , assimilation is usually limited by RcPc.

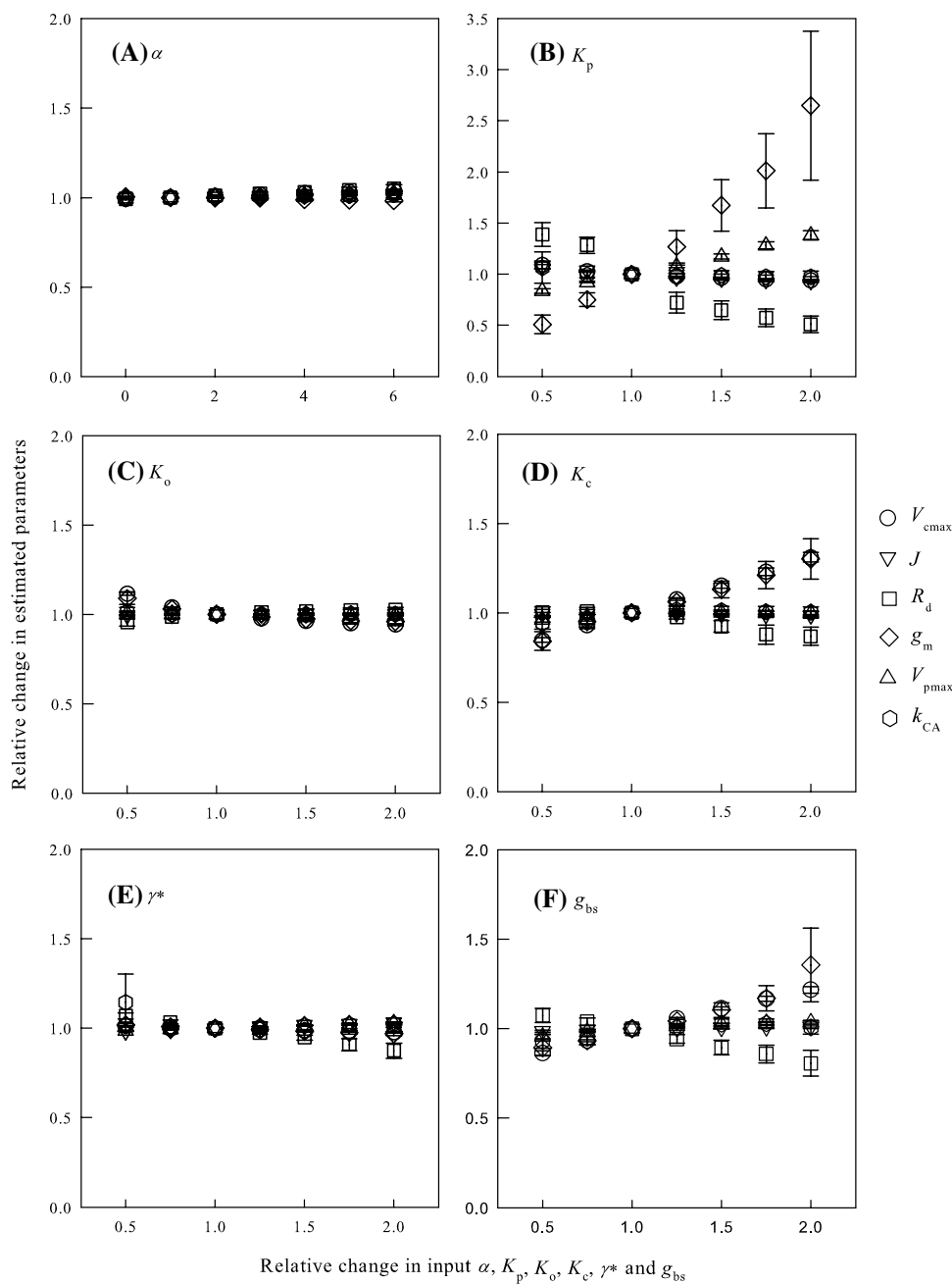
Sensitivity analysis

The parameters K_c , K_o , γ^* , K_p , α , and g_{bs} can vary among species in nature (Cousins et al. 2010; Galmés et al. 2016) and it is therefore important to know how sensitive our results are to variation in these parameters. We conducted a sensitivity analysis for variation in these parameters on the estimated V_{cmax} , J , R_d , V_{pmax} , g_m , and k_{CA} (Fig. 3). This analysis shows all the estimated parameters are robust under the variation of α (Fig. 3A) and showed little variation responding to the change of γ^* (Fig. 3E) and K_o (Fig. 3C); however, the estimated parameters are sensitive to other input parameters to different extents (Fig. 3B, D, F). We calculate the average percentage change of estimated parameters along with the 50% decrease and 100% increase of the input parameters. V_{cmax} showed sensitivity for K_c and g_{bs} with the average percentage change of 23.11 and 17.69% respectively but was relatively robust for K_p (7.54%). J is robust in the variations of K_c , and g_{bs} (the average change is less than 2%) and with a medium 6.96% change for K_p . k_{CA} is robust in the variations of K_c , K_p , and g_{bs} (average change less than 5%). V_{pmax} is sensitive for K_p with the average change of 27.34%, moderately sensitive to the decrease and increase of g_{bs} with 4.01% and 13.38% change respectively and is robust for K_c . R_d is sensitive to K_c , K_p , and g_{bs} with the average change of 6.73, 43.88 and 13.38%. g_m is strongly sensitive to K_c , K_p , and g_{bs} with the average percentage changes of 22.95, 107.04 and 23.19%. These results suggest that V_{cmax} , J , V_{pmax} , and k_{CA} estimated using our method are relatively robust.

Physiological significance for assimilation rate of the input parameters

In addition to the sensitivity analysis, we performed a simulation analysis to illustrate the physiological importance of input parameters further, and to indicate further the importance of physiological properties in maintaining the efficiency of C_4 photosynthesis pathway. We chose the estimation parameter set of *T. dactyloides* as an example, held photosynthetic parameters constant V_{cmax} ($28 \mu mol m^{-2} s^{-1}$), J ($134 \mu mol m^{-2} s^{-1}$), R_d ($0.78 \mu mol m^{-2} s^{-1}$), g_m ($30.00 \mu mol m^{-2} s^{-1} Pa^{-1}$), and V_{pmax} ($41.91 \mu mol m^{-2} s^{-1}$), while changing the values of α , γ^* , g_{bs} , and K_p (as half or twice of the original parameters) to see their effects on the assimilation rate, C_{bs} and the O_2 concentration in bundle sheath (O_{bs}) (Fig. 4; Table 2). Using photosynthetic parameter sets of other species to perform the simulation analysis yielded similar results (data not shown). The change of α did not lead to changes in assimilation rate (Fig. 4A) and led to small

Fig. 3 Sensitivity analysis of six estimation parameters to the variation in six input parameters using the model with carbonic anhydrase. Relative changes in the estimated V_{cmax} , J , R_d , V_{pmax} , g_m , and k_{CA} in response to the relative change of six input parameters (A α , B K_p , C K_o , D K_c , E γ^* , and F g_{bs}) from the initial values in Table S1. The relative change of estimated parameters refers to the ratio of estimated values at a changed input parameter to the estimated value at the initial value of that input parameter. The symbols represent the average change of the nine C_4 species and error bars represent standard error



changes in O_{bs} (Table 2). The decrease of γ^* to half of the current value led to a small change of C_{bs} and assimilation rate (less than $0.5 \mu\text{mol m}^{-2} \text{s}^{-1}$) while doubling γ^* led to a larger, but still not significant, change (less than $1 \mu\text{mol m}^{-2} \text{s}^{-1}$) (Fig. 4B; Table 2). Importantly, the changes of assimilation rates were less than $0.3 \mu\text{mol m}^{-2} \text{s}^{-1}$ when C_i was less than 20 Pa, which is the regular range of C_i under current ambient CO_2 . However, the change of g_{bs} significantly changed the assimilation rate and C_{bs} (Fig. 4C; Table 2). The change of K_p significantly affected the assimilation rate and C_{bs} to a large degree under low C_i (Fig. 4D; Table 2).

Validating the estimation methods

In order to test our estimation methods, we first conducted a simulation test with manipulated error terms. We use the estimated results of the nine species as known parameters (the known values in Fig. 5) to generate new datasets using the C_4 photosynthesis equations based the first assumption of electron transport and adding error terms to the assimilation rates. The error terms were randomly drawn from a normal distribution of mean zero and standard deviation of 0.1 or 0.2 in an effort to simulate the inevitable random errors in the real measurements. Estimating simulated data

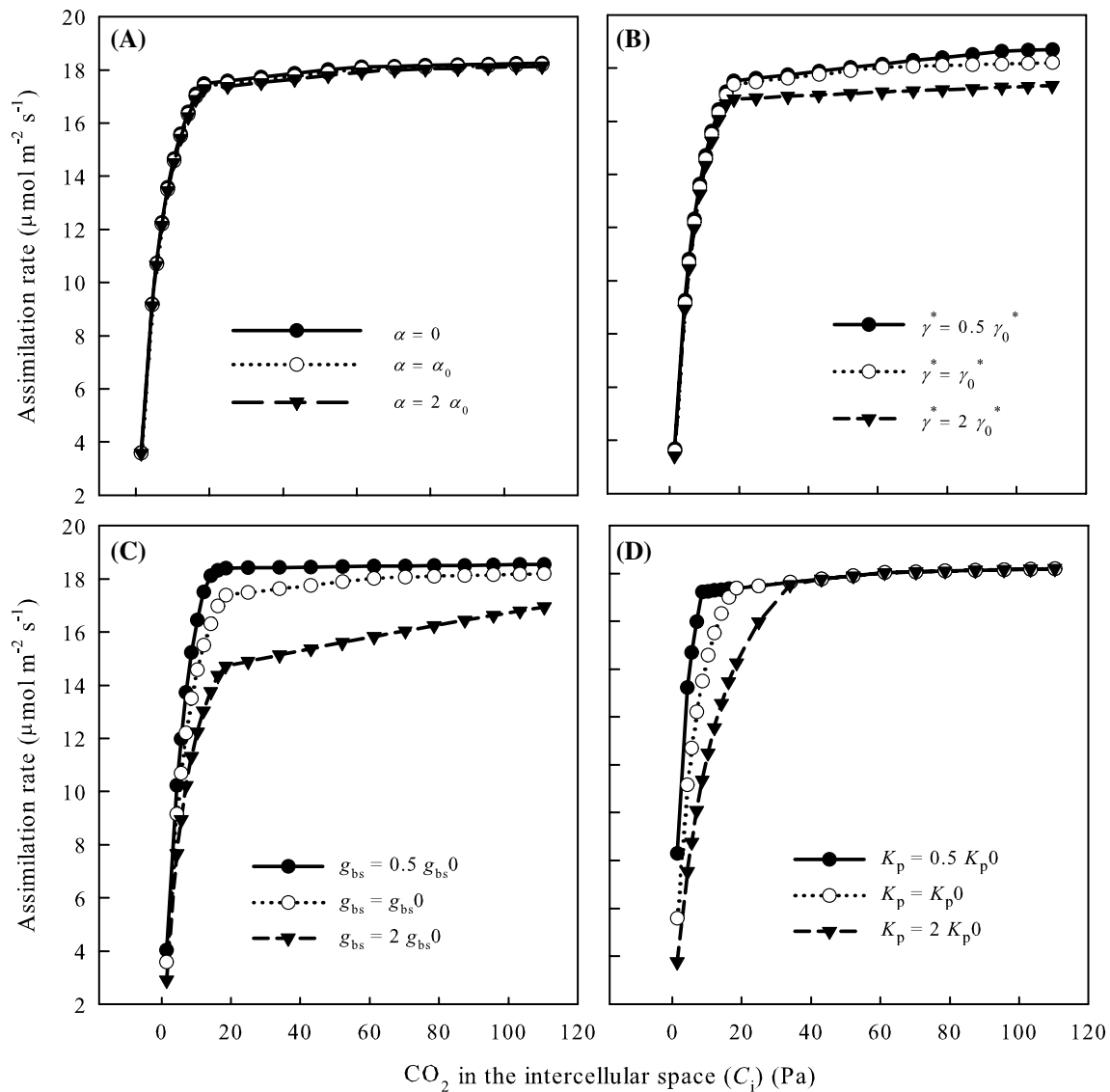


Fig. 4 Simulation results of assimilation rate along with different intercellular CO₂ concentration (C_i) with the known photosynthetic parameters, but with the change of **A** α, **B** γ*, **C** g_{bs} and **D** K_p. The original data set are V_{cmax} = 28 μmol m⁻² s⁻¹, J = 134 μmol m⁻² s⁻¹,

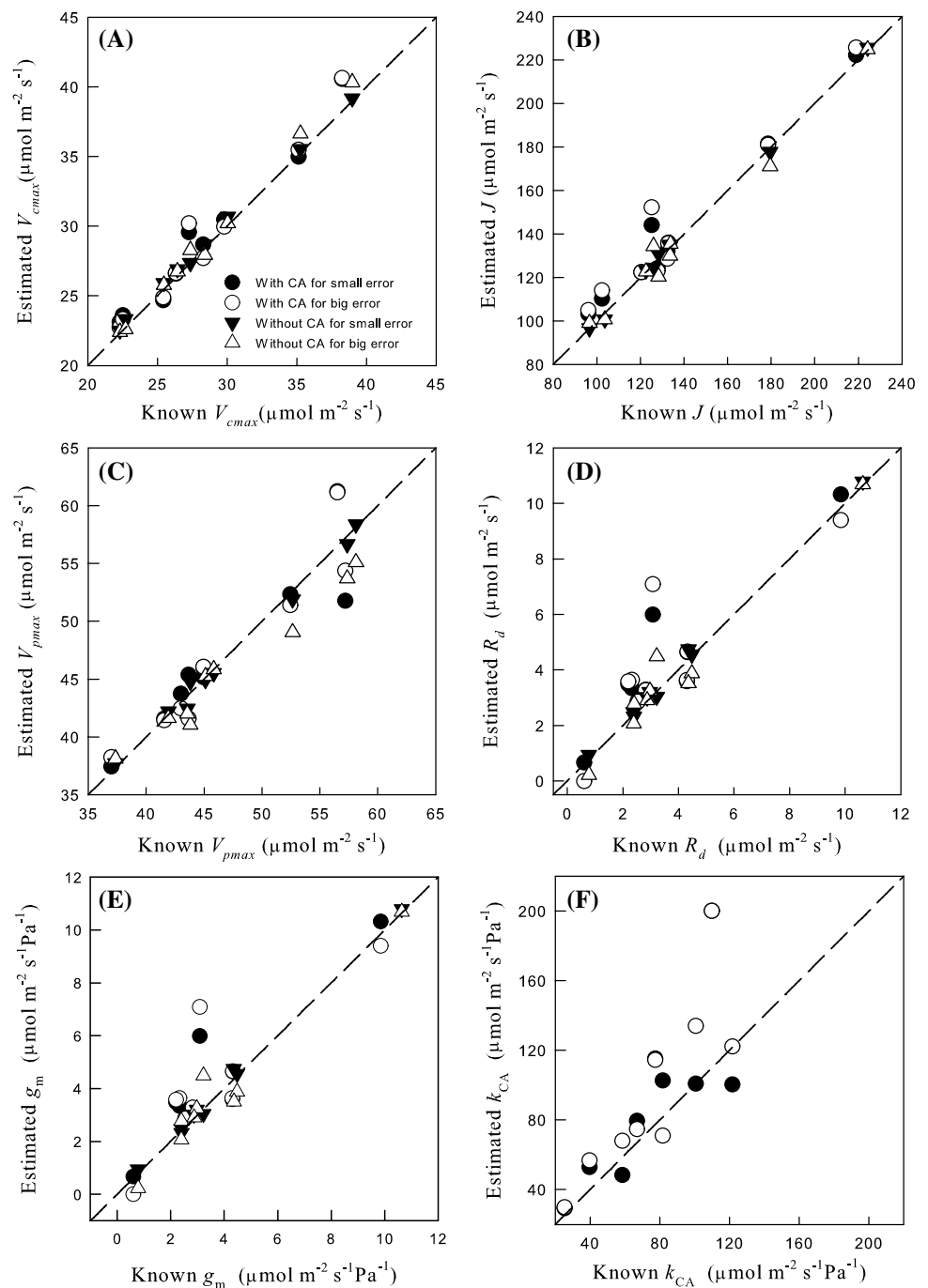
R_d = 0.78 μmol m⁻² s⁻¹, g_m = 30.00 μmol m⁻² s⁻¹ Pa⁻¹ and V_{pmax} = 41.91 μmol m⁻² s⁻¹. The reference value of changing parameters at 25 °C: α₀(25) = 0.15, γ*₀(25) = 0.000244, g_{bs0}(25) = 0.0295 and K_p(25) = 8.55 Pa

Table 2 The average change of percentage of CO₂ concentration (C_{bs}) and O₂ concentration at bundle sheath (O_{bs}) compared to the reference value of α₀, γ*₀, g_{bs0} and K_p

Parameters	α = 0	α = 2 α ₀	γ* = 0.5 γ* ₀	γ* = 2 γ* ₀
Change of C _{bs} (%)	-0.91(0.06)	0.97(0.06)	-2.96(0.28)	5.05(0.49)
Change of O _{bs} (%)	-6.07(0.30)	6.01(0.30)	0.07(0.01)	-0.21(0.02)
Parameters	g _{bs} = 0.5 g _{bs0}	g _{bs} = 2 g _{bs0}	K _p = 0.5 K _{p0}	K _p = 2 K _{p0}
Change of C _{bs} (%)	56.99(3.03)	-29.48(0.41)	43.12(10.75)	-36.57(4.07)
Change of O _{bs} (%)	6.77(0.29)	-3.41(0.16)	0.91(0.18)	-1.18(0.14)

Simulation results are obtained by using the original parameter set of *T. dactyloides* with V_{cmax} = 28 μmol m⁻² s⁻¹, J = 134 μmol m⁻² s⁻¹, R_d = 0.78 μmol m⁻² s⁻¹, g_m = 30.00 μmol m⁻² s⁻¹ Pa⁻¹ and V_{pmax} = 41.91 μmol m⁻² s⁻¹. The values represent average change of percentage of 21 values from 0 to 120 Pa of intercellular CO₂ (C_i) [data show mean (standard error)]

Fig. 5 Simulation tests for the estimated parameters (**A** V_{cmax} , **B** J , **C** V_{pmax} , **D** R_d , **E** g_m , and **F** k_{CA}) using estimation methods with and without carbonic anhydrase reaction (With CA and Without CA). Datasets are generated by adding random errors for the modeling results using the known photosynthesis parameters of nine species. These known photosynthesis parameters are the true values in the x-axis and are used to compare with the newly estimation parameters. The small error refers to error term randomly chosen with mean 0 and standard deviation of 0.1 and the bigger error refers to error term with randomly chosen mean 0 and standard deviation of 0.2. The line in the figure shows the 1:1 line



sets gave us an idea about how likely we can capture the real parameters of the species given unavoidable errors in measurements. The results show that robust estimation results for V_{cmax} , J , V_{pmax} , and R_d can be obtained (Fig. 5A, B, C, D). However, some estimation results of g_m and k_{CA} show some deviation from the real values (Fig. 5E, F).

To test whether our estimation method could give accurate predictions across typical prediction scenarios, (CO_2 ranging from 20 to 60 Pa), we performed out of sample tests for our nine target species. To perform these tests, we

removed five points of CO_2 concentrations between 20 and 60 Pa range out of the A/C_i curves and used the rest of the A/C_i curves to estimate parameters. And then we used these parameters to predict the assimilation rate under the CO_2 concentrations we took out before and calculated the estimation errors. In general, the estimation errors for all our species were small (Table 3).

We tried to compare our estimation methods with in vitro measurements or other estimation methods using isotopic analysis, especially for *Zea*. Our estimation results for *Zea*

Table 3 Out of sample test results

Species	<i>A. virginicus</i>	<i>Z. mays</i>	<i>E. trichodes</i>	<i>P. virgatum</i>	<i>P. amarum</i>
Model without CA	0.069 (0.036)	0.150 (0.056)	0.035 (0.017)	0.193 (0.063)	0.055 (0.034)
Model with CA	0.066 (0.043)	0.154 (0.057)	0.111 (0.058)	0.195 (0.061)	0.054 (0.033)
Species	<i>S. scoparium</i>	<i>S. faberi</i>	<i>S. nutans</i>	<i>T. dactyloides</i>	
Model without CA	0.023 (0.010)	0.114 (0.055)	0.258 (0.080)	0.199 (0.090)	
Model with CA	0.105 (0.034)	0.068 (0.040)	0.263 (0.133)	0.200 (0.090)	

Five measured points from 20 to 60 Pa were taken out when we conducted the estimation process. Then the calculated assimilation rates under these five CO₂ concentrations were compared with the measured ones. The data show estimated error [(measured value-estimated value)²] between the calculated and measured assimilation rates [data show mean (standard error)]

obtained similar V_{cmax} with the in vitro estimated Rubisco activity of Pinto et al. (2014) ($33 \mu\text{mol m}^{-2} \text{s}^{-1}$); however, the estimated value for V_{pmax} is a little lower than the in vitro PEPC activity measurement ($83 \mu\text{mol m}^{-2} \text{s}^{-1}$) with a difference of around $20 \mu\text{mol m}^{-2} \text{s}^{-1}$. This discrepancy could be related to the aqueous environmental differences in vitro versus in vivo. For species of the Panicum family with NAD-ME subtype, *P. virgatum* and *P. amarum* in the current study and *P. coloratum* in Pinto et al. (2014), the estimated V_{cmax} and V_{pmax} are quite consistent with the in vitro measurements (V_{cmax} of $33 \mu\text{mol m}^{-2} \text{s}^{-1}$ and V_{pmax} of $42 \mu\text{mol m}^{-2} \text{s}^{-1}$). Ubierna et al. (2017) reported the g_{m} for *Zea* ranged from 1.69 ± 0.17 to $8.19 \pm 0.80 \mu\text{mol m}^{-2} \text{s}^{-1} \text{Pa}^{-1}$ using ¹⁸O and in vitro V_{pmax} . Our estimation method fitted a g_{m} for *Zea* of $7.34 \mu\text{mol m}^{-2} \text{s}^{-1} \text{Pa}^{-1}$, which falls into the range of their measurements. Barbour et al. (2016) reported a higher mesophyll conductance of $17.8 \mu\text{mol m}^{-2} \text{s}^{-1} \text{Pa}^{-1}$ for *Zea* using ¹⁸O measurements.

Validating transition point range

We used chlorophyll fluorescence measurements from seven C₄ species to test whether the upper and lower boundary CO₂ concentrations, *CaL* and *CaH*, are reasonable (Table 4). The apparent quantum efficiency of

PSII electron transport was calculated with $\Delta F/Fm' = (Fm' - Fs) / Fm'$ (Genty et al. 1989). Fluorescence analysis (Baker et al. 2007) is a powerful tool for identifying the limitation states of C₃ species (Sharkey et al. 2007). If Chlorophyll fluorescence is increasing with increasing CO₂, A_n is limited by Rubisco carboxylation rate; when Chlorophyll fluorescence stays constant with increasing CO₂, A_n is limited by RuBP regeneration. For C₄ species, however, the situation is more complicated. Since V_p could be limited by V_{pr} and V_{pc} (Eq. (9) in Supplementary Methods). Part of the RuBP carboxylation limited condition and RuBP regeneration limited condition for the C₃ cycle will mix together, leading to a linear increase of fluorescence with increasing of CO₂, but of a small slope (Fig. S2). Thus, we can only obtain two boundaries of CO₂ concentrations. Below the lower boundary, A and fluorescence increases with increasing C_i with a steep slope and A is RuBP carboxylation and PEP carboxylation limited (RcPc); above the higher boundary, A and fluorescence is relatively constant along with the increase of C_i and A is RuBP regeneration and PEP regeneration limited (RrPr). We measured fluorescence to test whether the upper and lower boundary CO₂ concentrations, *CaL* and *CaH*, are reasonable. It seems all the *CaL* are above 14 Pa and all the *CaH* are below 65 Pa (Table 4). These results suggest that 10–65 Pa is a reasonable range for the transitional point.

Table 4 CO₂ concentration boundaries result for assimilation-limited conditions from fluorescence measurements for seven species

Species	<i>P. virgatum</i>	<i>P. amarum</i>	<i>S. scoparium</i>	<i>S. nutans</i>
Low (Pa)	14.1 (1.12)	18.0 (1.09)	17.8 (1.09)	17.6 (0.28)
High (Pa)	34.1 (1.78)	55.5 (1.40)	53.1 (1.10)	63.1 (2.07)
Species	<i>T. dactyloides</i>	<i>T. flavus</i>	<i>B. mutica</i>	
Low (Pa)	13.8 (0.35)	14.9 (2.35)	15.8 (1.13)	
High (Pa)	46.1 (0.20)	41.4 (1.73)	42.3 (1.24)	

Low: CO₂ concentration under which assimilation rate increases greatly with increasing CO₂ (potentially assimilation is limited by PEP carboxylation and RuBP carboxylation). High: CO₂ concentration above which assimilation rate no longer increases with increasing CO₂ (potentially assimilation is limited by PEP regeneration and RuBP regeneration). Data show the mean (standard error)

Discussion

The photosynthetic parameters from the estimation method are good indicators for the biochemical and biophysical mechanisms underlying the photosynthesis processes of plants. Together with photosynthesis models, they can provide powerful information for evolutionary and ecological questions in both physiological and ecosystem response to natural environmental variation and climate change, to illustrate evolutionary trajectory of C_4 pathway, as well as in efforts to improve crop productivity (Osborne and Beerling 2006; Osborne and Sack 2012; Heckmann et al. 2013). Photosynthetic parameters represent different physiological traits, and comparison of these parameters within a phylogenetic background could help us to understand the further divergence of lineages and species through evolutionary time. Additionally, the response of productivity and carbon cycle of vegetation towards the future climate change depends heavily on photosynthesis parameter estimation as input parameters.

Each of the two different fitting procedures has advantages and disadvantages. Yin's method (Supplementary material II) uses the explicit calculation of assimilation rate and consequently gives lower estimation error. However, it needs a more accurate assignment of limitation states, especially at the lower end. Thus, Yin's method will be preferable if one has additional support (e.g., fluorescence measurements) to define the limitation states; otherwise, the Yin's method may give unbalanced results (Fig. 3). However, Sharkey's method (Supplementary material I) usually can avoid unbalanced results even without ancillary measurements. Thus, it is better to use both procedures to support each other to find more accurate results. For example, one can first use Sharkey's method to get estimation results and limitation states, and then use them as initial values for Yin's method.

Our estimation methods yielded similar results when using models with and without carbonic anhydrase reaction processes. Although carbonic anhydrase activity may well be a limiting step for C_4 cycle (von Caemmerer et al. 2004; Studer et al. 2014; Boyd et al. 2015; Ubierna et al. 2017), its limitation did not greatly affect assimilation rates in this study. Including the carbonic anhydrase reaction makes the model more complex and difficult to get an explicit solution; therefore, the model without carbonic anhydrase could be used as a simplified form yielding flawed but 'nearly correct' predicted values as a part of larger models. However, carbonic anhydrase limitation of C_4 photosynthesis needs the further assessment from physiological or biochemical perspectives, and our estimation method provides another way to derive carbonic anhydrase parameters, which were comparable with *in vitro* measurements (Boyd et al. 2015). It is possible if a

machine with better low CO_2 control (e.g., Li-cor 6800) is used, carbonic anhydrase may become more limiting at extremely low CO_2 concentrations. In addition, our results for models with and without carbonic anhydrase activity support the proposition of Cousins et al. (2007) that carbonic anhydrase activity may not be a limiting factor for A/C_i curves of C_4 plants.

Our results show that despite a clear difference between the assumptions of how the products of electron transport are distributed, the results were similar and comparable with studies using different models under measurements of high light intensity. The bump in the second model happens in RrPc. In RrPc, assimilation is limited by RuBP regeneration and PEP carboxylation; therefore, PEP regeneration is not reaching V_{pr} , and the extra electron transport in PEP regeneration could be freely assigned to RuBP regeneration. This effect will weaken as PEP carboxylation increases. However, under lower photosynthetic photon flux density, assimilation rate will be limited more by electron transport, and the separate assumptions concerning electron transport may start to show divergent results. Such divergence of predictions under low or high light could provide a way to test assumptions about electron transport further in the future. Such a test should be done for multiple species as different species may follow different assumptions.

It is worth highlighting other assumptions that upon which our estimation methods rely. First, our estimation methods share with previous methods an underlying assumption that dark and light reactions optimally co-limit the assimilation rate (Sharkey et al. 2007; Yin et al. 2011b; Ubierna et al. 2013; Bellasio et al. 2015). This requires that there is some kind of optimization of nitrogen allocation of RuBP carboxylation and RuBP regeneration. The optimality assumption is intuitive as there should be some mechanism to balance the resource distribution between dark and light reactions to avoid inefficiency. Nonetheless, it is possible that there is redundancy in nitrogen allocation in one reaction, which can cause the photosynthesis rate to be always limited by the dark or light reactions. Second, we did not differentiate between C_4 subtypes in our model as we assumed electron transport is limited by ATP production and there is a similar ATP cost for different C_4 subtypes (Hatch 1987). Such an assumption can be relaxed further to build exclusive estimation methods for different subtypes by considering mechanistic details. Third, we assumed the parameters, K_c , K_o , γ^* , K_p , α , and g_{bs} to be the same for different species. To get more accurate estimation results, one can use species-specific parameters obtaining from other measurements.

Researchers need to pay additional attention to interpret the estimated parameters. For the electron transport, J , our methods do not assume saturated light intensity. Instead, J is defined as maximal electron transport for the specific light intensity under which the A/C_i curve is obtained. Using our

estimation methods, one can estimate “realized” J at different light intensities (e.g., a light intensity encountered by plants in natural habitat, but light intensity should not be very low because A/C_i curve may not be reliable). To estimate maximal electron transport rate for saturated light (J_{\max}), one can obtain the A/C_i curve under saturated light condition, where the “realized” J would be equal to the J_{\max} . A similar statement also applies to the estimation of V_{cmax} . It is possible that low light intensity may not maximize the Rubisco activation state. Thus, in such conditions, the estimation methods would estimate “realized V_{cmax} ” under a specific light intensity, instead of the real V_{cmax} . Such interpretations for estimated parameters also pertain to the previous estimation methods. Similar with other C_4 estimation methods (Yin et al. 2011b; Ubierna et al. 2013; Bellasio et al. 2015), we did not estimate the triose phosphate utilization (TPU). TPU has been found to limit assimilation rate when the A/C_i curve reaches a plateau and show a little decrease in C_3 (Sharkey et al. 2007). Since we did not detect a decrease in our measurements and it is not clear how TPU affects C_4 assimilation, we did not take it into consideration. However, TPU does deserve further consideration in future studies.

The photosynthetic parameters from the estimation method used together with photosynthesis models can provide information and inspiration about the evolutionary and physiological importance of different aspects of the C_4 syndrome (Osborne and Sack 2012; Heckmann et al. 2013), which can be investigated by empirical measurements. Several examples emanate from our simulation analysis: (1) α represents the fraction of O_2 evolution from photosynthesis occurring in the bundle sheath cells [Eq. (4) in Supplementary Methods] and any $\alpha > 0$ means that O_2 will accumulate in the bundle sheath cells, due to low g_{bs} . Both the sensitivity analysis and the simulation analysis showed the change of α did not affect the estimated parameters and assimilation rates, because the high C_{bs} created by C_4 carbon concentrating mechanism overcame any increase of O_{bs} and did not lead to high photorespiration. Thus, the compartmentation of O_2 evolution may not have played an important role in the evolution of C_4 photosynthesis. (2) A lower Rubisco specificity factor [γ^* ; Eq. (11) in Supplementary Methods] means lower specificity for O_2 , higher specificity for CO_2 , and lower photorespiration. In C_3 species, selection for Rubisco with lower specificity to O_2 and high specificity of CO_2 can increase the carbon gain. However, there is a trade-off between the specificity of Rubisco for CO_2 and its catalytic rate (Savir et al. 2010; Studer et al. 2014). Based on this trade-off, we can hypothesize that since C_4 elevates CO_2 around Rubisco relative to the O_2 concentration, maintaining low specificity might be optimal, in order to get high catalytic rate of the enzyme to reach higher assimilation rate as shown by the empirical measurements of Sage (2002)

and Savir et al. (2010). Our simulation analysis showed the increase of specificity for CO_2 (decrease of γ^*) did not increase the assimilation rate much, which indicates the selection upon Rubisco specificity in C_4 plants should be relaxed. (3) g_{bs} represents CO_2 leakage from bundle sheath to the mesophyll cell, and changes in g_{bs} significantly change the assimilation rate and C_{bs} . Therefore, avoiding CO_2 leakage was of great importance for the evolution and efficiency of C_4 photosynthesis pathway (Brown and Byrd 1993; Ubierna et al. 2013; Kromdijk et al. 2014).

Although we have shown that parameter estimation can be achieved solely with A/C_i curves, it is easy to combine our methods with ancillary measurements to yield more accurate estimation results by defining the parameters as estimated or known or add additional constraints (Supplementary Material IV). Yin et al. (2011b) proposed a method to obtain R_d from the fluorescence-light curve, since the method used for C_3 species, the Laik method, is inappropriate (Yin et al. 2011a). Additional measurement of dark respiration could be an approximation for R_d or could help to provide a constraint for estimating R_d in our estimating method. Ubierna et al. (2017) discussed the estimation method of g_m using instantaneous carbon isotope discrimination. With external measurement results, one can change estimated parameters (such as R_d , g_m and J) as input parameters, instead of output parameters, in this curve fitting method (Supplementary material IV). Additional methods, such as in vitro measurements (Boyd et al. 2015; Pedomo et al. 2015) and membrane inlet mass spectrometry (Cousins et al. 2010) of V_{cmax} , V_{pmax} , and carbonic anhydrase activity can also provide potential parameter values. Furthermore, if some output parameters are determined in the external measurements, one can also relax the input parameters (such as g_{bs}) and make them estimated parameters (Supplementary material IV).

Conclusion

We have developed new, accessible estimation tools for extracting C_4 photosynthesis parameters from intensive A/C_i curves. Our estimation method is based on an established estimation protocol for C_3 plants and makes several improvements upon C_4 photosynthesis models. External measurements for specific parameters will increase the reliability of estimation methods and are summarized independently. We developed estimation methods with and without carbonic anhydrase activity. The comparison of these two methods allows for an estimation of carbonic anhydrase activity, and further shows that the method that did not consider carbonic anhydrase activity was a sufficient simplification for C_4 photosynthesis. We tested two assumptions related to whether the electron transport is freely distributed between RuBP regeneration and PEP regeneration or certain proportions are

confined to the two mechanisms. They show similar results under high light. Simulation test, out of sample test, fluorescence analysis, and sensitivity analysis confirmed that our methods gave robust estimation especially for V_{cmax} , J , and V_{pmax} .

Acknowledgements We are grateful for support from the University of Pennsylvania. We thank Dr. Jesse Nippert, Kansas State University, for providing the fluorometer chamber.

Funding We sincerely thank the constructive comments from two anonymous reviewers. The experiments are supported by Department Research Fund (to H.Z.) from Department of Biology, University of Pennsylvania.

Compliance with ethical standards

Conflict of interest The authors declare that they have no conflict of interest.

References

- Baker NR, Harbinson J, Kramer DM (2007) Determining the limitations and regulation of photosynthetic energy transduction in leaves. *Plant Cell Environ* 30:1107–1125
- Barbour MM, Evans JR, Simonin KA, Von Caemmerer S (2016) Online CO_2 and H_2O oxygen isotope fractionation allows estimation of mesophyll conductance in C_4 plants, and reveals that mesophyll conductance decreases as leaves age in both C_4 and C_3 plants. *New Phytol* 210:875–889
- Bellasio C, Burgess SJ, Griffiths H, Hibberd JM (2014) A high throughput gas exchange screen for determining rates of photorespiration or regulation of C_4 activity. *J Exp Bot* 65:3769–3779
- Bellasio C, Beerling DJ, Griffiths H (2015) Deriving C_4 photosynthetic parameters from combined gas exchange and chlorophyll fluorescence using an Excel tool: theory and practice. *Plant Cell Environ*. <https://doi.org/10.1111/pce.12626>
- Boyd RA, Gandin A, Cousins AB (2015) Temperature responses of C_4 photosynthesis: biochemical analysis of Rubisco, phosphoenolpyruvate carboxylase, and carbonic anhydrase in *Setaria viridis*. *Plant Physiol* 169:1850–1861
- Brown RH, Byrd GT (1993) Estimation of bundle sheath cell conductance in C_4 species and O_2 insensitivity of photosynthesis. *Plant Physiol* 103:1183–1188
- Chi Y, Xu M, Shen R, Yang Q, Huang B, Wan S (2013) Acclimation of foliar respiration and photosynthesis in response to experimental warming in a temperate steppe in northern China. *PLoS ONE* 8:e56482
- Cousins AB, Baroli I, Badger MR, Ivakov A, Lea PJ, Leegood RC, von Caemmerer S (2007) The role of phosphoenolpyruvate carboxylase during C_4 photosynthetic isotope exchange and stomatal conductance. *Plant Physiol* 145:1006–1017
- Cousins AB, Ghannoum O, von Caemmerer S, Badger MR (2010) Simultaneous determination of Rubisco carboxylase and oxygenase kinetic parameters in *Triticum aestivum* and *Zea mays* using membrane inlet mass spectrometry. *Plant Cell Environ* 33:444–452
- Dubois JB, Fiscus EL, Booker FL, Flowers MD, Reid CD (2007) Optimizing the statistical estimation of the parameters of the Farquhar-von Caemmerer-Berry model of photosynthesis. *New Phytol* 176:402–414
- Ethier GJ, Livingston NJ, Harrison DL, Black TA, Moran JA (2006) Low stomatal and internal conductance to CO_2 versus Rubisco deactivation as determinants of the photosynthetic decline of ageing evergreen leaves. *Plant Cell Environ* 29:2168–2184
- Farquhar GD, von Caemmerer S, Berry JA (1980) A biochemical model of photosynthetic carbon dioxide assimilation in leaves of 3-carbon pathway species. *Planta* 149:78–90
- Galmés J, Hermida-Carrera C, Laanisto L, Niinemets U (2016) A compendium of temperature responses of Rubisco kinetic traits: variability among and within photosynthetic groups and impacts on photosynthesis modeling. *J Exp Bot* 67:5067–5091
- Genty B, Briantais J, Baker N (1989) The relationship between the quantum yield of photosynthetic electron transport and quenching of chlorophyll fluorescence. *Biochim Biophys Acta* 990:87–92
- Gu L, Pallardy SG, Tu K, Law BE, Wullschlegel SD (2010) Reliable estimation of biochemical parameters from C_3 leaf photosynthesis-intercellular carbon dioxide response curves. *Plant Cell Environ* 33:1852–1874
- Hatch MD (1987) C_4 photosynthesis: a unique blend of modified biochemistry, anatomy and ultrastructure. *Biochim Biophys Acta* 895:81–106
- Hatch MD, Burnell JN (1990) Carbonic anhydrase activity in leaves and its role in the first step of C_4 photosynthesis. *Plant Physiol* 93:825–828
- Heckmann D, Schulze S, Denton A, Gowik U, Westhoff P, Weber AP, Lercher MJ (2013) Predicting C_4 photosynthesis evolution: modular, individually adaptive steps on a Mount Fuji fitness landscape. *Cell* 153:1579–1588
- Jenkins CLD, Furbank RT, Hatch MD (1989) Mechanism of C_4 photosynthesis. A model describing the inorganic carbon pool in bundle-sheath cells. *Plant Physiol* 91:1372–1381
- Kromdijk J, Ubierna N, Cousins AB, Griffiths H (2014) Bundle-sheath leakiness in C_4 photosynthesis: a careful balancing act between CO_2 concentration and assimilation. *J Exp Bot* 65:3443–3457
- Miao ZW, Xu M, Lathrop RG, Wang YF (2009) Comparison of the A- C_c curve fitting methods in determining maximum ribulose 1,5-bisphosphate carboxylase/oxygenase carboxylation rate, potential light saturated electron transport rate and leaf dark respiration. *Plant Cell Environ* 32:1191–1204
- Osborne CP, Beerling DJ (2006) Nature's green revolution: the remarkable evolutionary rise of C_4 plants. *Philos Trans R Soc B* 361:173–194
- Osborne CP, Sack L (2012) Evolution of C_4 plants: a new hypothesis for an interaction of CO_2 and water relations mediated by plant hydraulics. *Philos Trans R Soc B* 367:583–600
- Pedomo JA, Cavanagh AP, Kubien DS, Galmes J (2015) Temperature dependence of *in vitro* Rubisco kinetics in species of *Flaveria* with different photosynthetic mechanisms. *Photosynth Res* 124:67–75
- Pinto H, Sharwood RE, Tissue DT, Ghannoum O (2014) Photosynthesis of C_3 , $\text{C}_3\text{-C}_4$, and C_4 grasses at glacial CO_2 . *J Exp Bot* 65:3669–3681
- Sage RF (2002) Variation in the k_{cat} of Rubisco in C_3 and C_4 plants and some implications for photosynthetic performance at high and low temperature. *J Exp Bot* 53:609–620
- Savir Y, Noor E, Milo R, Tlustý T (2010) Cross-species analysis traces adaptation of Rubisco toward optimality in a low-dimensional landscape. *Proc Natl Acad Sci USA* 107:3475–3480
- Sharkey TD, Bernacchi CJ, Farquhar GD, Singaas EL (2007) Fitting photosynthetic carbon dioxide response curves for C_3 leaves. *Plant Cell Environ* 30:1035–1040
- Studer RA, Christin PA, Williams MA, Orengo CA (2014) Stability-activity tradeoffs constrain the adaptive evolution of Rubisco. *Proc Natl Acad Sci USA* 111:2223–2228
- Ubierna N, Sun W, Kramer DM, Cousins AB (2013) The efficiency of C_4 photosynthesis under low light conditions in *Zea mays*.

- Miscanthus X giganteus* and *Flaveria bidentis*. *Plant Cell Environ* 36:365–381
- Ubierna N, Gandin A, Boyd RA, Cousins AB (2017) Temperature response of mesophyll conductance in three C_4 species calculated with two methods: ^{18}O discrimination and in vitro V_{pmax} . *New Phytol* 214:66–80
- von Caemmerer S (2000) Biochemical models of photosynthesis. In: *Techniques in plant sciences*. CSIRO Publishing, Colingwood, p 196
- von Caemmerer S, Quinn V, Hancock NC, Price GD, Furbank RT, Ludwig M (2004) Carbonic anhydrase and C_4 photosynthesis: a transgenic analysis. *Plant Cell Environ* 27:697–703
- Xu LK, Baldocchi DD (2003) Seasonal trends in photosynthetic parameters and stomatal conductance of blue oak (*Quercus douglasii*) under prolonged summer drought and high temperature. *Tree Physiol* 23:865–877
- Yin X, Struik PC, Romero P, Harbinson J, Evers JB, Van Der Putten PEL, Vos JAN (2009) Using combined measurements of gas exchange and chlorophyll fluorescence to estimate parameters of a biochemical C_3 photosynthesis model: a critical appraisal and a new integrated approach applied to leaves in a wheat (*Triticum aestivum*) canopy. *Plant Cell Environ* 32:448–464
- Yin X, Sun Z, Struik PC, Gu J (2011a) Evaluating a new method to estimate the rate of leaf respiration in the light by analysis of combined gas exchange and chlorophyll fluorescence measurements. *J Exp Bot* 62:3489–3499
- Yin XY, Sun ZP, Struik PC, Van der Putten PEL, Van Ieperen W, Harbinson J (2011b) Using a biochemical C_4 photosynthesis model and combined gas exchange and chlorophyll fluorescence measurements to estimate bundle-sheath conductance of maize leaves differing in age and nitrogen content. *Plant Cell Environ* 34:2183–2199

Publisher's Note Springer Nature remains neutral with regard to jurisdictional claims in published maps and institutional affiliations.